Special Issue

Speciation of Copper(II)-Betaine Complexes as Starting Point for Electrochemical Copper Deposition from Ionic Liquids

Janine Richter,[a] Maximilian Knies,[a] and Michael Ruck*[a, b]

The application of ionic liquids for the dissolution of metal oxides is a promising field for the development of more energy- and resource-efficient metallurgical processes. Using such solutions for the production of valuable chemicals or electrochemical metal deposition requires a detailed understanding of the chemical system and the factors influencing it. In the present work, several compounds are reported that crystallize after the dissolution of copper(II) oxide in the ionic liquid [Hbet][NTf_2]. Dependent on the initial amount of chloride, the reaction temperature and the purity of the reagent, copper crystallizes in complexes with varying coordination geometries and ligands. Subsequently, the influence of these different complex species on electrochemical properties is shown. For the first time, copper is deposited from the ionic liquid [Hbet][NTf_2], giving promising opportunities for more resource-efficient copper plating. The copper coatings were analyzed by SEM and EDX measurements. Furthermore, a mechanism for the decomposition of [Hbet][NTf_2] in the presence of chloride is suggested and supported by experimental evidence.

1. Introduction

Metal oxides play a significant role in many industrially important processes. On one side, they are employed as starting materials in terms of ores, earths and minerals used for metal production. These conventional processes typically use temperatures around 1000 °C, making the production of the respective metal very energy-consuming and CO_2-emitting due to the prevalence of fossil fuels.[1] On the other side, metal oxides appear as waste in many industrial processes.[2–5] The recovery of these important resources is conventionally realized by hydrometallurgical processing, generating large amounts of contaminated waste water.[6]

A currently investigated approach to overcome these problems is the application of reusable non-aqueous solvents such as ionic liquids (ILs)[7–14] or deep-eutectic solvents (DESs).[15–23] Referring to hydrometallurgy, we suggest the term *ionometallurgical processing* for metal extraction by means of ILs and DESs.

A detailed overview about the dissolution of metal oxides in ILs and DESs is given in a recent review,[24] whereas only a few important examples will be mentioned here. While DESs are cheaper to produce and less toxic than ILs, their dissolution abilities have not yet been able to match those of ILs.[24] Although ILs can be toxic and can require considerable effort in their production, they are regarded as green solvents. This is due to their negligible vapor pressure, preventing inhalation and diffusion into the atmosphere. Their non-flammability contributes to safe handling. Furthermore, ILs enable many reactions that do not happen in other solvents.[25] Thus, they are promising chemicals for developing greener, more resource- and energy-efficient processes.

First dissolutions of metal oxides were reported in chloroaluminate ILs, formed by the mixing of an organic salt and $AlCl_3$.[12,26–28] These ILs are suitable to provide strong interactions to metal atoms, hence supporting the dissolution of the oxides. However, the hygroscopic $AlCl_3$ causes the ILs' decomposition in the presence of air and moisture.[25] In order to overcome this disadvantage, air-stable ILs with discrete anions, such as bis(trifluoromethylsulfonyl)imide ($[NTf_2]^-$), were applied. As these anions are typically weakly coordinating, the interactions to metal atoms supporting dissolution have to be provided by the cations of the ILs or by additives.[11,29] As the potential of conventional ILs in this field is limited, task-specific ILs (TSIL) were applied to the dissolution of metal oxides. These are often air- and water-stable ILs featuring a functional group, e.g. a carboxyl group that can be deprotonated to a chelating ligand.[25] Moreover, their protons can form water with the oxygen of the metal oxide. Different carboxyl[30] as well as sulfonic,[31] sulfamic[10] or alkylsulfuric[9] acid-functionalized TSIL were reported, whereby even rather inert metal oxides could be dissolved.

[a] J. Richter, M. Knies, Prof. Dr. M. Ruck
Faculty of Chemistry and Food Chemistry
Technische Universität Dresden
01062 Dresden (Germany)
E-mail: michael.ruck@tu-dresden.de
[b] Prof. Dr. M. Ruck
Max Planck Institute for Chemical Physics of Solids
01187 Dresden (Germany)

Supporting information for this article is available on the WWW under https://doi.org/10.1002/open.202000231

Special Issue *An invited contribution to a Special Issue dedicated to Material Synthesis in Ionic Liquids*

An example of TSILs, intensively studied in recent research, is betainium bis(trifluoromethylsulfonyl)imide, [Hbet][NTf_2]. Despite exhibiting a lower solubility than ILs with sulfurous acid groups, [Hbet][NTf_2] has the advantage of betaine being a natural byproduct of sugar production.[32] Thus, the cation is highly available and the effort for its synthesis is low. The dissolution of the solid is driven by water formation, as the carboxylic protons react with the oxide anions, as well as the formation of stable metal-betaine complexes.[33] *Nockemann* et al. initiated the research on [Hbet][NTf_2], investigating solutions that contained additional water. The water molecules were found to support the dissolution reaction of metal oxides by acting as supporting ligands of smaller size next to the sterically demanding betaine.[33,34] *Binnemans* et al. discovered that the dissolution of metal oxides is also possible in water-free [Hbet][NTf_2], and that chloride ions can support the reaction.[4] This observation was confirmed by extensive investigations of our group on the dissolution of numerous metal oxides in water-free [Hbet][NTf_2] or [Hbet]$_2$[NTf_2]Cl, which is the equimolar mixture of the IL and its chloride salt [Hbet]Cl. In the course of these studies, the decomposition of the IL [Hbet][NTf_2] in the presence of chloride became apparent, without the mechanism being resolved.[35]

However, the dissolution in [Hbet][NTf_2] cannot be the final point in the processing of metal oxides. Instead, starting from these solutions, the production of desired chemicals by downstream chemistry or electrochemical metal deposition are consequent next steps. An essential condition for the latter is the stability of the medium during electrolysis. This often limits the applicability of common, easy to handle laboratory solvents, such as water or acetone, especially when non-precious metals are to be deposited.[36,37] Here, ILs appear to be a suitable alternative with generally very large electrochemical windows, typically 3 V to 6 V. However, it has to be taken into account that many factors, especially impurities, influence electrochemical windows.[38,39] The electrodeposition of lithium[12] and lead[40] from ILs as well as copper,[41,42] nickel,[43] lead[20,21,44] and zinc[23,45–48] from DESs was reported after the dissolution of the respective metal oxide. Lead[40] and plutonium[49] were already deposited from [Hbet][NTf_2].

The metal copper is a widely used coating material, e.g. for protective coatings in machine components or conductive layers in circuit boards.[50] Such coatings, are typically applied via electroplating, whereby a copper anode is oxidized.[51] Besides the need to produce such anodes, environmental problems are caused by the large amounts of water used for the aqueous electrolyte, concomitant with wastewater, as well as the high demand of electrical energy for the process and for heating.[52] Significant improvements might be achievable by the usage of ILs for copper plating. Instead of expensively producing electrodes of metallic copper, a more efficient process could be the dissolution of oxidic copper minerals (tenorite) or CuO from pyrometallurgy and the subsequent direct electrodeposition of copper.

Copper was deposited from different ILs during the last decades, whereby only a few examples will be mentioned, here. *Endres* and *Schweizer* reduced copper from $CuCl_2$ dissolved in the basic IL 1-butyl-3-methylimidazolium chloride/aluminum chloride ([bmim]Cl/$AlCl_3$) on Au(111) films and highly ordered pyrolytic graphite. Due to the air sensitivity of the IL, all experiments had to be performed under inert gas atmosphere.[53] *Chen* and *Sun* compared the copper deposition from 1-ethyl-3-methylimidazolium chloride tetrafluoroborate ([emim]·Cl·[BF_4]) on tungsten, platinum and glassy carbon under argon and ambient atmosphere, showing very similar behavior. In ambient atmosphere, the IL absorbs some moisture, however, the electrochemical windows, 4.5 V or 3.2 V as a subject of IL composition, are not affected.[54] *Fricoteaux* et al. deposited copper on a nickel surface in a chloride-free system from the IL 1-butyl-1-methylpyrrolidinium bis-(trifluoromethylsulfonyl)imide ([bmpyrr][NTf_2]).[55] Apparently, in ILs, copper is deposited via one-electron transfer steps with Cu^+ existing as dissolved intermediate.[53–55]

For metal electrodeposition, it is important to know about the metal-containing species present in the solution as electrochemical potentials depend on the coordination environment of the metal ion. This was recently discussed by *Abbott* et al. for electrochemical copper deposition from DESs.[56] In this work, we describe several complex compounds that were obtained by the dissolution of copper(II) oxide in [Hbet][NTf_2] together with the reaction parameters influencing the product speciation. Furthermore, we demonstrate that the electrodeposition of copper from these solutions is possible and suggest a mechanism for the chloride-assisted decomposition of [Hbet][NTf_2]. With this study, we aim to give a proof of concept on the dissolution of copper(II) oxide in [Hbet][NTf_2] and the subsequent electrodeposition of copper. The complexity of this process shall be discussed in order to establish a basis for future optimization and to transfer the process to other metal systems more easily.

2. Results and Discussion

In the course of the dissolution of copper(II) oxide in [Hbet][NTf_2], the following reaction conditions were varied: the chloride ion concentration and the temperature as well as the purity of the used CuO. The structures of four coordination compounds, which were obtained as crystalline products, were determined with single-crystal X-ray diffraction (SCXRD). Previous studies on rare earth metal-betaine complexes gave evidence for the dissociation of crystallized binuclear complexes into dissolved mononuclear units.[57] Therefore, we cannot be certain about the dissolved and the crystallized complex species being the same. Nonetheless, the crystal structures should provide evidence for diverse processes taking place. This is expected to affect further steps in downstream chemistry and electrodeposition.

2.1. $[Cu_2(bet)_4(NTf_2)_2][NTf_2]_2$

The complex compound $[Cu_2(bet)_4(NTf_2)_2][NTf_2]_2$ **1** was previously reported as the first metal-betaine complex without water

molecules in the metal atom's coordination sphere. The cationic complex is a paddle wheel, in which two copper(II) ions are coordinated by four μ-bridging betaine ligands and two weakly O-coordinating $[NTf_2]^-$ anions (Figure 1).[35]

$[Cu_2(bet)_4(NTf_2)_2][NTf_2]_2$ was synthesized by reacting copper (II) oxide and $[Hbet][NTf_2]$ in the molar ratio of 1:2 at 175 °C. Furthermore, evidence for a catalytic effect of chloride ions was found as the addition of small amounts of [Hbet]Cl resulted in a significant reduction of the reaction time. Thus, the product in the maximum yield of 66% is obtained after 100 h without [Hbet]Cl, but after only 24 h with the addition of 0.3 mol % [Hbet]Cl.[35] The product is obtained regardless of the purity of the starting material, i.e. from 99.995% as well as 97.5% copper (II) oxide.

2.2. $[Cu(bet)_4]_2[N(CH_3)_3(CH_2Cl)][NTf_2]_5$

Based on the observations made in synthesizing **1**, we further investigated the influence of chloride ions, this time when added in stoichiometric amounts. For this purpose, copper(II) oxide, $[Hbet][NTf_2]$ and [Hbet]Cl were heated to 175 °C in the molar ratio of 1:2:2. This ratio was chosen because the excess of betaine ligands towards the metal cations did never exceed 1:4 in previously reported metal-betaine complexes.[33,34] At the same time, enough chloride was supplied to complete a potentially octahedral coordination sphere, as is common for copper(II). The time for the complete dissolution of copper(II) oxide was reduced to four hours only.

The blue rod-like crystals were identified as the complex compound $[Cu(bet)_4]_2[N(CH_3)_3(CH_2Cl)][NTf_2]_5$ **2**, crystallizing in the monoclinic space group $P2_1/n$ (no. 14) with the lattice parameters $a = 2109.56(9)$ pm, $b = 2232.56(9)$ pm, $c = 2181.44(9)$ pm, and $\beta = 90.633(1)°$ at 100 K.

The compound consists of two cationic $[Cu(bet)_4]^{2+}$ complexes, one $[N(CH_3)_3(CH_2Cl)]^+$ cation and five $[NTf_2]^-$ anions (Figure S1, Supporting Information). In the complex cation, displayed in Figure 2, copper(II) is coordinated by four monodentate betaine ligands via oxygen. The coordination of copper (II) is square planar, formed by four oxygen atoms in equal distances [194.6(2)–195.6(2) pm]. The *cis* angles between two adjacent betaine ligands range from 89.5(1)° to 90.9(1)° and the *trans* angles between two opposing ligands from 176.9(1)° to 179.1(1)°.

In literature, monomeric square-planar copper-carboxylate complexes appear to be rather rare, as the paddle-wheel conformation is favored. *Nockemann* et al. reported the complex cation $[Cu(bet)_4(H_2O)_2]^{2+}$ in the compound $[Cu(bet)_4(H_2O)_2][Cu_2(bet)_4(H_2O)_2][NTf_2]_6$.[33] The distances between copper(II) and the oxygen atoms of the coordinating betaine ligands (194.2–195.4 pm) are rather similar to those reported here. However, in *Nockemann*'s compound two additional water molecules coordinate to copper(II). Therefore, its copper(II) ion is in octahedral coordination, unlike the $[Cu(bet)_4]^{2+}$ complex in **2**.

The $[Cu(bet)_4]^{2+}$ cations in **2** are loosely arranged in pseudo-chains along the crystallographic *b* direction. There are no distinct interactions between the chains, such as hydrogen bridges, and they are separated by $[NTf_2]^-$ anions. Furthermore, the crystal structure contains $[N(CH_3)_3(CH_2Cl)]^+$ cations, which must be a fragment of decomposed betaine. This cation was already reported earlier,[58–64] however, air-sensitivity of the compound due to the decomposition of the cation, as suggested by *Johnson* et al.,[64] was not observed here.

The decomposition of the IL $[Hbet][NTf_2]$ in the presence of larger amounts of chloride, was already noted previously.[35] Taking the crystallographic observation of $[N(CH_3)_3(CH_2Cl)]^+$ into account, a suggestion regarding the decomposition mechanism can be made, as shown in Scheme 1.

As a first step in a mixture of $[Hbet][NTf_2]$ and [Hbet]Cl, we suggest the formation of chlorine according to the Deacon reaction. In the presence of protons (from the $[Hbet]^+$ carboxyl group), chloride ions are oxidized to chlorine by atmospheric oxygen.[65] This mechanistic suggestion is in agreement with

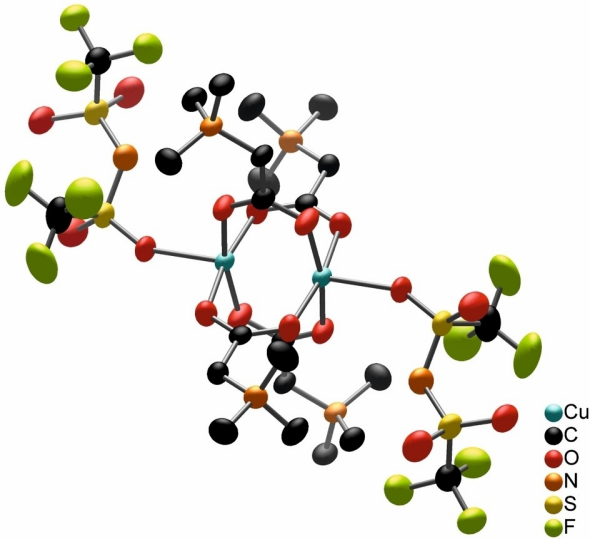

Figure 1. $[Cu_2(bet)_4(NTf_2)_2]^{2+}$ cation as observed in the crystal structure of **1**. The ellipsoids enclose 75% of the probability density of the atoms at 100 K. H atoms are omitted for clarity.

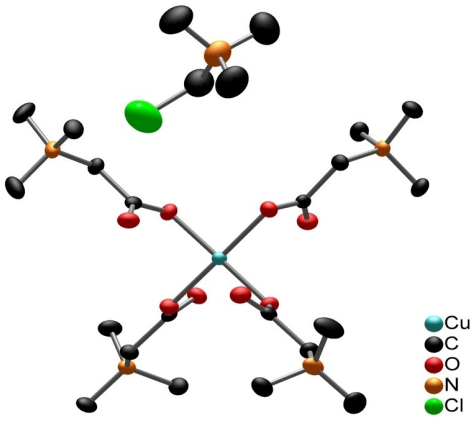

Figure 2. $[Cu(bet)_4]^{2+}$ and $[N(CH_3)_3(CH_2Cl)]^+$ cations as observed in the crystal structure of **2**. The ellipsoids enclose 75% of the probability density of the atoms at 100 K. H atoms are omitted for clarity.

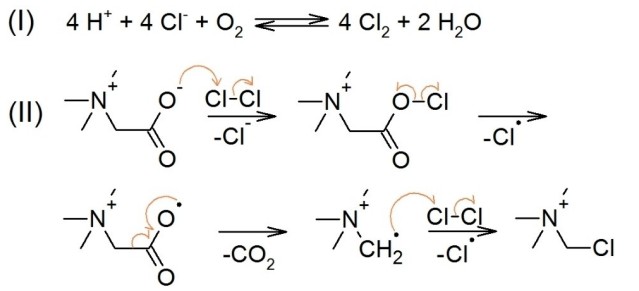

Scheme 1. Proposed decomposition mechanism of the IL [Hbet][NTf_2] in the presence of chloride. The reaction is assumed to take place according to (I) a Deacon process and (II) a Hunsdieker reaction.

experimental proof for the presence of chlorine by the reduction of iodide ions (Figure S4).

Subsequently, the decomposition of the IL could take place according to a Hunsdieker reaction.[66,67] Thermally induced and analogous to the disproportionation of chlorine in basic conditions, the asymmetric cleavage of chlorine-chlorine bonds takes place. Via a radical decarboxylation, carbon dioxide evolves. Recombination of the diradical pair $[N(CH_3)_3(CH_2\cdot)]^+$ and Cl· or the radical cleavage of a chlorine molecule yields $[N(CH_3)_3(CH_2Cl)]^+$. This suggested mechanism is in agreement with experimental proof for carbon dioxide evolution by conducting the reaction gas phase through lime water (Figure S4). Furthermore, in IR spectra, a shift in the band of the asymmetric stretching vibration ν_{as} of COOH supports the suggested mechanism.[35] With a radical mechanism, $[N(CH_3)_3(CH_2Cl)]^+$ should not be the only decomposition product, but a number of substances might be present in solution.

This decomposition process of the IL is assumed to be thermally induced. However, for a Deacon as well as a Hunsdieker reaction, metal ions are usually assumed to be necessary as catalyst.[1,66,68] Therefore, the reaction taking place in a mixture of [Hbet][NTf_2] and [Hbet]Cl without any metal salts added, might be attributed to ILs generally featuring impurities, as well. On one side, [Hbet]Cl has a purity of only 99%, on the other side, there might still be lithium ions contained in the IL originating from its synthesis (metathesis reaction of [Hbet]Cl and Li[NTf_2]).[69]

2.3. $[Cu_3(bet)_4Cl_3][NTf_2]_3$

$[Cu_3(bet)_4Cl_3][NTf_2]_3$ **3** was found in a long-time crystallization experiment of a mixture of copper(II) oxide (99.995%), [Hbet][NTf_2], and [Hbet]Cl with the molar ratio of 1:6:1, which was stored at room temperature for nine months in an open vessel. After the observations of the decomposition of the IL by chloride, we varied the ratio of the reagents in order to reduce or avoid this reaction. Compound **2** also showed that chloride supports the dissolution of copper(II) oxide, but does not necessarily act as ligand in the precipitated complex, for what reason its amount was reduced with respect to copper(II). Within the first two days after the sample preparation, green and yellow coloring occurred at several spots in the powders. During the next months, color change to green and yellow advanced in the whole sample. No additional characterization was performed during this time as probing might have changed the composition of the remaining sample. When no further color change could be noticed for several weeks, the sample was investigated in detail under the microscope. The greenish product contained particles of several shapes and colors, of which a crystal was identified as **3**.

Compound **3** crystallizes in the polar orthorhombic space group $Cmc2_1$ (no. 36) with the lattice parameters $a = 2504.27(9)$ pm, $b = 1661.29(6)$ pm, and $c = 1342.53(5)$ pm at 100 K (Figure S2). The structure consists of positively charged infinite chains of $[Cu_3(bet)_4Cl_3]^{3+}$ units in c direction, as displayed in Figure 3. These chains are separated from each other by non-coordinating $[NTf_2]^-$ anions.

The copper(II) atoms in the cationic chain have three different coordination environments and are connected by bridging betaine and chlorido ligands. According to charge balance $[(4\times\pm0)_{bet}+(3\times-1)_{Cl-}+(3\times-1)_{[NTf2]-}= -6]$, every copper atom occupies the oxidation state +II. Cu1 and Cu2 exhibit a square pyramidal coordination environment with chloride in the axial position. While Cu1 is additionally coordinated by two chlorido and two betaine ligands in equatorial positions, the square plane around Cu2 is formed by four betaine ligands. The angles between the axial and the equatorial ligands [Cu1 96.5(1) –105.5(1)°, Cu2 97.0(1) –102.3(1)°] indicate a significant distortion from square-pyramidal geometry. With axial *trans* angles significantly smaller than 180° [Cu1 157.8(1)°, Cu2 160.7(1)°] the copper(II) atoms clearly are not positioned in the base of the pyramids. This is attributed to attractive interactions of copper(II) and the axial ligand. In contrast, Cu3 shows almost square-planar coordination by two

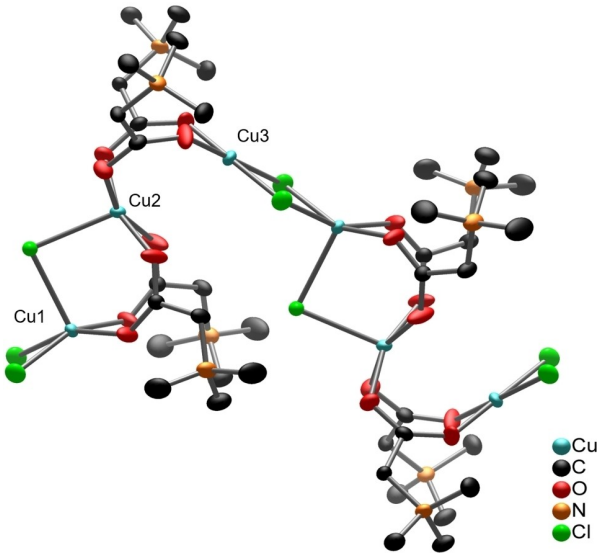

Figure 3. Section of the $[Cu_3(bet)_4Cl_3]^{3+}$ cationic chain as observed in the crystal structure of **3**. The ellipsoids enclose 75% of the probability density of the atoms at 100 K. H atoms are omitted for clarity.

chlorido and two betaine ligands [*cis* angles 88.1(1)° – 90.8(1)°, *trans* angles 178.7(1)°].

For all copper atoms, almost equal distances to coordinating betaine oxygen atoms are found [193.6(2)–197.1(2) pm]. These values are in the same range as in previously reported monomeric and dimeric copper betaine complexes.[33,35] For chloride, shorter distances to copper are present in equatorial positions (226.5–231.3 pm) and longer distances in axial positions (243.4–246.4 pm). As the copper–copper distances (≥ 317.8 pm) are at least 21% larger than in the copper paddle wheel of **1** (262.7 pm),[35] no significant interactions between the copper atoms are assumed.

Copper(II) in distorted square-pyramidal coordination of chloride and oxygen atoms wasalso reported as anionic polymer strand in several compounds for a $[Cu^{II}O_2Cl_3]$ coordination environment[70] and in $[Cu(C_2H_7N_5)_2][Cu(C_5H_7O_2)_2Cl]_2$[71] for $[Cu^{II}O_4Cl]$. Copper(II)–oxygen distances (191.7–205.8 pm) and copper(II)–chloride distances (225.4–230.3 pm) in equatorial positions are similar to the complex $[Cu_3(bet)_4Cl_3]^{3+}$, however, the distances between copper and chloride in the axial position are significantly longer in literature (258.1–278.3 pm). A main difference is, that only bridging chloride ions are present in **3**, which is not the case in the literature compounds. This weakens the bonding of equatorial chlorido ligands and allows a shorter distance between copper and chloride in the axial position.

For the square-planar coordinated Cu3, similar copper(II)–oxygen distances [193.6(2) pm] and copper(II)–chloride distances [226.5(1) pm] as in the equatorial planes of Cu1 and Cu2 are found. These values are in good agreement with other complexes with copper(II) in a square-planar coordination by two oxygen and two chloride atoms, such as $[C_5H_4N_2O_2]_2[Cu(H_2O)_2Cl_2]$ (195.0 pm and 226.6 pm)[72] and $[Cu(C_{18}H_{34}O_4N_2)Cl_2]$ (194.0 pm and 228.5 pm).[73] Similar to the compound reported herein, only minor deviations from 90° *cis* and 180° *trans* angles appear.

$[NTf_2]^-$ ions are arranged between the cationic chains, parallel to *a* or to *b* direction.

2.4. $[Cu_2(bet)_4][Cu_6Cl_{10}]$

After different reaction outcomes were observed when 99.995% or 97.5% pure copper(II) oxide were used, $[Cu_2(bet)_4][Cu_6Cl_{10}]$ **4** was synthesized the same way as **2**, yet with the difference of less pure copper(II) oxide (97.5%) as starting material. No impurities were detected in the reagent by powder X-ray diffraction (PXRD). The treatment of the substance in an oxygen stream at 500 °C, in order to oxidize potentially contained copper(I) oxide, did not lead to a change in reactivity. Thus, the nature of the 2.5% impurities remains undetermined.

Complex compound **4** crystallizes in the monoclinic space group $P2_1/n$ (no. 14) with the lattice parameters $a = 1516.32(14)$ pm, $b = 906.38(8)$ pm, $c = 1652.66(16)$ pm, and $\beta = 113.018(3)°$ (Figure S3). The structure consists of uncharged infinite chains arranged parallel to each other, which can formally be separated into cationic and anionic sections (Figure 4).

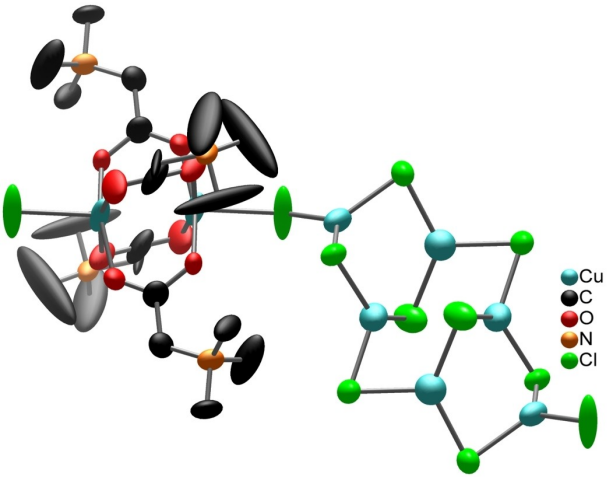

Figure 4. Section of the $[Cu_2(bet)_4][Cu_6Cl_{10}]$ chain as observed in the crystal structure of **4**. The ellipsoids enclose 75% of the probability density of the atoms at 100 K. H atoms are omitted and for split atoms, only one position is shown for clarity.

The formally positively charged part $[Cu_2(bet)_4]^{4+}$ is a copper paddle wheel. Four betaine ligands are μ-bridging coordinated to two copper(II) ions with similar copper–oxygen distances [184.6(9) –213.5(12) pm]. In average, this is in good agreement with $[Cu_2(bet)_4(NTf_2)_2][NTf_2]_2$, whereby the wider range of distances is attributed to disorder. The octahedral coordination sphere around each copper(II) atom is completed by one coordinating chloride ion and the neighboring copper atom. The copper–chloride distance amounts to 244.2(2) pm, while the distance between two copper(II) atoms is 269.2(2) pm.

The atoms of the betaine ligands show large displacement ellipsoids indicating disorder. To restrict the complexity of the structure model, split positions were refined for two oxygen atoms only. As a result, a wide range of ligand *cis* angles is found [61.9(8)–101.1(6)°]. The *trans* angles significantly deviating from planarity [157.6(5)–164.1(3) pm] indicate a distortion from pseudo-octahedral coordination, attributed to relatively strong copper(II)-chloride interactions These distances and angles are in very good agreement with the complex cation $[Cu_2(bet)_4Cl_2]^{2+}$ in the compound $[Cu_2(bet)_4Cl_2]Cl \cdot 4H_2O$.[74]

The coordinating chloride is provided by the formally anionic $[Cu_6Cl_{10}]^{4-}$ part. In this fragment, every copper atom is coordinated by three chloride atoms, forming two six-membered rings, which are annulated with a central eight-membered ring. According to charge balance $[(4\times\pm0)_{bet}+(2\times+2)_{Cu}+(10\times-1)_{Cl-}=-6]$, the copper atoms are present in the oxidation state +I. This is in accordance with the low coordination number and the trigonal coordination, which is (besides tetrahedral coordination) typical for copper(I). Shorter copper(I)–chloride distances [221.9(2)–235.5(2) pm] compared to the copper(II) –chloride bond in the paddle wheel [244.2(2) pm] as well as bond valance sums between 0.91 and 1.05[75] strongly support this assumption. A similar situation was observed in the mixed valence copper compound $[Cu(C_4H_6N_2)_4][CuCl_3]\cdot H_2O$. There, copper(I) is coordinated by three chloride ions with distances of 222.4–225.9 pm, while the coordination

sphere of copper(II) consists of a distorted square of four nitrogen atoms and perpendicular to this two chlorido ligands in a distance of 292.2 pm and 300.7 pm.[76] The $[Cu_6Cl_{10}]^{4-}$ structure fragment of **4** was previously found in the compounds $[Cu(C_5H_{12}N_2)_2]_2[Cu_6Cl_{10}]$[77] and $[N(C_2H_5)_4]_3[Cu_7Cl_{10}]$[78] with similar copper(I)–chloride distances (220.4-231.1 pm).[77,78] Similar to **4**, $[Cu_6Cl_{10}]^{4-}$ acts as bridging ligand for two copper(II) atoms. Thus, the first compound is a neutral complex,[77] while in the second compound, $[Cu_6Cl_{10}]^{4-}$ entities are connected by copper (II) atoms, forming negatively charged infinite chains.[78]

2.5. Influence of Reaction Parameters

With the four crystal structures discussed, a significant influence of the reaction conditions on the crystallized copper-betaine complex after the dissolution of copper(II) oxide in [Hbet][NTf_2] becomes apparent.

As reported before, chloride ions do not only show a catalytic effect on the dissolution reaction and the formation of **1**,[35] but in larger quantities **2** is obtained as product. In **2**, chloride ions do not act as ligands to copper, however, they appear to have a structure-directing effect. As *Nockemann* et al. showed that complex speciation differs in dissolved and crystallized metal-betaine complexes,[57] chloride might occupy coordination sites in the dissolved complex, but crystallization in this form is not favored.

On the other hand, compound **3**, with betaine and chloride forming three different coordination spheres around copper(II), is obtained at room temperature from a slightly altered reaction mixture. This structure shows that chloride can act as a ligand in copper-betaine complexes under suitable reaction conditions. Reasons could be the influence of entropy or the different amount of ions in solution.

Similarly, by dissolving copper(II) oxide of lower purity, compound **4** gives evidence for other impurities influencing the reaction as well. Copper in the oxidation state +I might be part of these impurities, however, oxidizing the starting material in an oxygen stream did not influence the reaction or the product. Therefore, a redox reaction also is possible.

Thus, three factors on complex speciation in the copper-betaine system were identified: chloride content, reaction temperature and impurities. As the crystallized products in this system often show a relatively wide variety of crystal shapes and colors (in different shades of yellow, green and blue), the four complexes reported here, are not assumed to be the only ones existing. However, they shall serve as examples for the dependence of complex species on reaction conditions.

2.6. Electrochemical Copper Deposition

Having achieved some knowledge about different variables influencing complex speciation in the system of copper(II) oxide and betaine, we investigated their influence on the electrodeposition of copper. As impurities usually complicate electrochemical systems, these studies were limited to copper(II) oxide of 99.995 % purity as reagent.

Three samples of (A) pure [Hbet][NTf_2], (B) copper(II) oxide and [Hbet][NTf_2] as well as (C) copper(II) oxide, [Hbet][NTf_2] and [Hbet]Cl were investigated. These three samples have quite different appearance and properties. (A) The IL [Hbet][NTf_2] is a solid at room temperature and melts at 57 °C.[33] (B) From copper(II) oxide and [Hbet][NTf_2], compound **1** crystallizes almost instantly, giving a solid even at 175 °C. (C) In contrast, the mixture of copper(II) oxide, [Hbet][NTf_2] and [Hbet]Cl gives a liquid at 175 °C, from which crystals precipitate after several hours at room temperature. Moreover, the IL in this sample slowly decomposes at this elevated temperature.

In order to allow comparable studies at room temperature, a suitable, preferable green solvent had to be found. For more information on the investigated solvents, see Table S4. (B) is soluble in water, methanol, ethanol, ethylene glycol, acetone, acetonitrile and sulfolane. Low or negligible solubility is found in *i*-propanol, *n*-butanol and ethyl acetate. (C) dissolves in each of these solvents, whereas in the most samples not yet identified green-blue precipitations occur. The reflections in the PXRD pattern of the precipitates (Figure S5) cannot be attributed to any known substance, however, their colors suggest copper(II) compounds. Furthermore, the PXRD patterns indicate, that in the aprotic solvents acetone and acetonitrile, the same precipitate was obtained. The same is true for the alcohols and ethyl acetate. This is in agreement with IR spectra (Figure S6), where several bands in every spectrum are attributed to betaine. However, the high intensity bands of the $[NTf_2]^-$ anion are only observed in the spectra of the alcohol and ethyl acetate precipitations. Furthermore, ν_{as}(COO) is not or very weakly observed at 1770 cm^{-1} as expected for uncoordinated $[Hbet]^+$. Instead, bands shifted to lower wave numbers occur, suggesting the coordination of betaine.[35] These observations suggest a precipitated copper-betaine coordination compound free of $[NTf_2]^-$ anions for the acetone and acetonitrile precipitations, but $[NTf_2]^-$-containing or -associated copper-betaine complexes for the precipitations in the other solvents. Furthermore, several additional bands compared to pure [Hbet][NTf_2] suggest the presence of other organic components.

Although, the samples can be dissolved in alcohols, we aimed at an aprotic solvent as the presence of protons, hence the possibility of the protonation of betaine ligands, might affect the copper(II)-betaine complexes. At the same time, the chosen solvent should have a wide electrochemical window in order to get the best conditions for electrodeposition. Having these requirements, acetonitrile and sulfolane were chosen as solvents for electrochemical investigations. Currently, sulfolane is a relatively uncommon solvent in electrochemistry. However, a recent report showed the electrodeposition of silicon from this solvent.[79] Furthermore, ternary mixtures of sulfolane, 3-methyl sulfolane and different ILs were used in high-temperature supercapacitors.[80] For our samples, sulfolane clearly is the better solvent as no precipitation occurs and it is suggested as a "recommended green solvent" by *Clark* et al. in a review comparing different solvent selection guides.[81] This is in agreement with other reports highlighting the low skin

penetration of sulfolane, presumably no mutagenic, clastogenic, carcinogenic or reproductive toxicity, its low volatility and its application to environmentally more benign processes.[82–85] However, with a boiling point of 287 °C,[82] the distillation of the solvent for the recycling of the IL will not be possible without its decomposition.[4] In contrast to this, in acetonitrile, a supposedly copper-containing precipitation occurs during the dissolution of the chloride-rich sample and it is suggested as a "problematic green solvent".[81] However, the dissolution takes place significantly faster and the boiling point of only 82 °C allows the easy separation of the solvent from the IL.

Cyclic voltammograms (CVs) of the three samples in acetonitrile are shown in Figure 5. From the CV of pure [Hbet][NTf_2] in acetonitrile, sample (A), it becomes apparent that at voltages below −1.0 V, electrochemical reactions of the solvent take place. Therefore, oxidation or reduction processes of the metal ions are difficult to analyze in this regime.

For sample (B), which contained copper(II) oxide and [Hbet][NTf_2], two anodic peaks are observed at −0.8 V and −1.7 V and two cathodic peaks at −0.7 V and −0.4 V. This might be the reversible two-stage reduction of copper(II) to copper(0) via copper(I). *Abbott* and *McKenzie* studied the CVs of different copper(II) salts in DESs and found that anodic and cathodic peaks for both redox couples Cu^{II}/Cu^{I} and Cu^{I}/Cu^{0} are observable. However, their electrochemical potentials depend on the anions and additional complexing agents present in the solution.[86] As the electrodeposition of copper from [Hbet][NTf_2] has not been reported before, an exact comparison cannot be made. Furthermore, the analysis of the electrochemical peaks is complicated by electrochemical reactions of the solvent below −1.0 V.

For the sample with a large amount of chloride (C), several small anodic peaks appear at 0.1 V and below −1.0 V and, therefore, should not be assigned to specific reactions. Two cathodic peaks are observed at −0.4 V and 0.3 V, which might result from the oxidation of copper(0) and copper(I).

Dissolving the samples in sulfolane, quite different CVs are obtained, as shown in Figure 6. In sample (A) with only [Hbet][NTf_2] dissolved, an anodic peak is observed at −1.1 V and a cathodic peak at 1.1 V. Therefore, it has to be taken into account that a reaction of [Hbet][NTf_2] in sulfolane or of the solvent itself takes place at these potentials. Accordingly, the respective peaks in samples (B) and (C) are attributed to the same process.

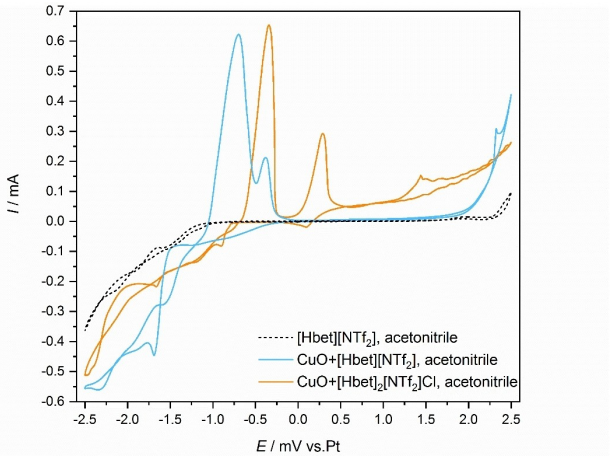

Figure 5. CVs of pure [Hbet][NTf_2] (A) and copper(II) oxide-[Hbet][NTf_2] mixtures in acetonitrile in the absence (B) and presence of chloride (C), recorded at room temperature at a scan rate of 10 mV/s.

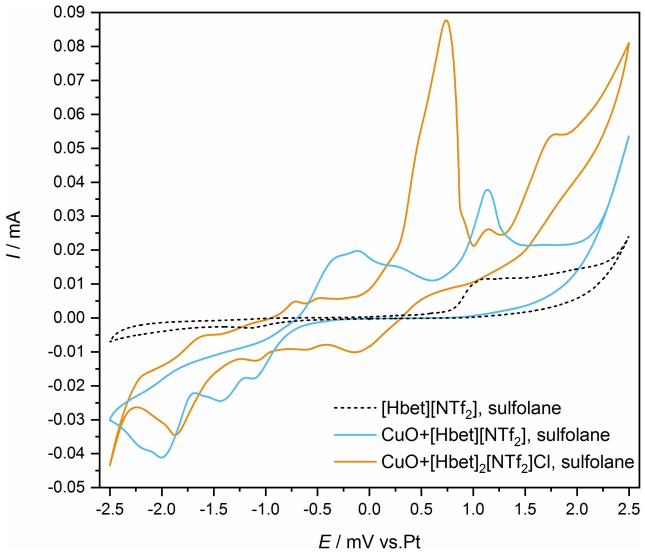

Figure 6. CVs of pure [Hbet][NTf_2] (A) and copper(II) oxide-[Hbet][NTf_2] mixtures in sulfolane in the absence (B) and presence of chloride (C), recorded at room temperature at a scan rate of 10 mV/s.

For sample (B), two additional anodic peaks at −1.4 V and −2.0 V as well as a broad cathodic peak at −0.1 V with a shoulder at 0.2 V are observed. In agreement with the same sample in acetonitrile, these peaks could be attributed to the reversible reduction of copper(II) to copper(0) via copper(I). As solvents influence electrochemical potentials, a difference between the CV signals in acetonitrile and sulfolane meets general expectations.

The CV of sample (C) in sulfolane is less clear as several anodic (−0.1 V, −0.6 V and −1.9 V) and cathodic peaks (−1.6 V, −0.7 V, −0.5 V, 0.7 V, 1.8 V) are observed. Apparently, electrochemical electron transfer reactions do not only involve copper in the presence of chloride, but other processes occur.

These CVs clearly show that sample composition and, therefore, complex speciation, has a significant effect on metal deposition potentials. Furthermore, complex speciation limits the options of sample preparation for electrochemical experiments. In the chloride-rich sample (C) dissolved in acetonitrile, a significant amount of the copper content is expected to be lost by precipitation. In order to compare the electrochemical behavior of different chloride-rich samples, a sample (D) of copper(II) oxide and [Hbet]Cl in an excess of aqueous [Hbet][NTf_2] without any organic solvent was prepared. *Nockemann* et al. showed that [Hbet][NTf_2], despite being hydrophobic, is able to take up approximately 14 wt. % of water at room temperature before phase separation occurs.[33] This content is assumed for the IL used here, which was freshly synthesized, but not dried. Despite water being problematic in electro-

chemistry, the advantages are a lowered viscosity and prevented crystallization. With copper being a noble metal, copper deposition without significant water decomposition is expected to be possible. However, the CV range had to be decreased to $-1.5\ V \leq E \leq 1.0\ V$ in order to reduce the electrolysis of water. As shown in Figure 7, two anodic peaks are observed at −0.6 V and −1.0 V as well as two cathodic peaks at −0.9 V and 0.2 V. These peaks are attributed to the reversible two-step reduction of copper(II). This CV differing significantly from the chloride-rich sample (C) in acetonitrile and sulfolane, is not surprising as electrochemical potentials depend on the chemical system. Compared to the organic solvent solutions, the aqueous sample (C) shows only the two anodic, respectively cathodic peaks, which are attributed to the redox couples Cu^{II}/Cu^{I} and Cu^{I}/Cu^{0}. Reducing the measuring range, therefore, could be useful to avoid other electrochemical reactions in the solvent samples as well. However, from these CVs it is not clear whether both copper reduction and oxidation steps take place in this potential range, as electrochemical reactions of pure [Hbet][NTf_2] in acetonitrile as well as sulfolane are observed.

Finally, we aimed on the macroscopic copper deposition as proof of concept for the direct copper plating from a copper(II) oxide solution in IL. A simple two-electrode cell was used, which is a cheap and easy to handle method for first electrodeposition experiments.[87,88] The copper coating of a steel electrode was investigated in six solutions. The steel surface was polished prior to use in order to remove contaminations and oxide layers as well as to enable optimal electrodeposition on a smooth steel surface. The effectivity of the cleaning procedure, i.e. the smoothening of the initially rough electrode surface, is evidenced by SEM pictures in Figure S7. The example of the chloride-rich sample in aqueous [Hbet][NTf_2] (D) already shows that the sample composition has to be adjusted in order to realize electrochemical metal deposition. Among other aspects, a suitable viscosity is required and the decomposition of the IL should be prevented as good as possible. The latter condition limits the range in which the viscosity can be regulated by increasing the temperature. One option for low-temperature optimization is the usage of water-containing [Hbet][NTf_2], which is, however, not favored due to the inconvenient electrochemical properties of water. Another option is an excess of [Hbet][NTf_2] in order to obtain copper-betaine complexes dissolved in unreacted IL. And, third, other suitable solvents could be added. Therefore, firstly, copper deposition was performed in the solution of copper(II) oxide and [Hbet]Cl in aqueous [Hbet][NTf_2] (D). Secondly, a water-free mixture of copper(II) oxide and [Hbet]Cl in [Hbet][NTf_2] (E) was investigated. Thirdly, mixtures of copper(II) oxide and [Hbet][NTf_2] with and without additional [Hbet]Cl dissolved in acetonitrile and sulfolane (B), (C) were studied.

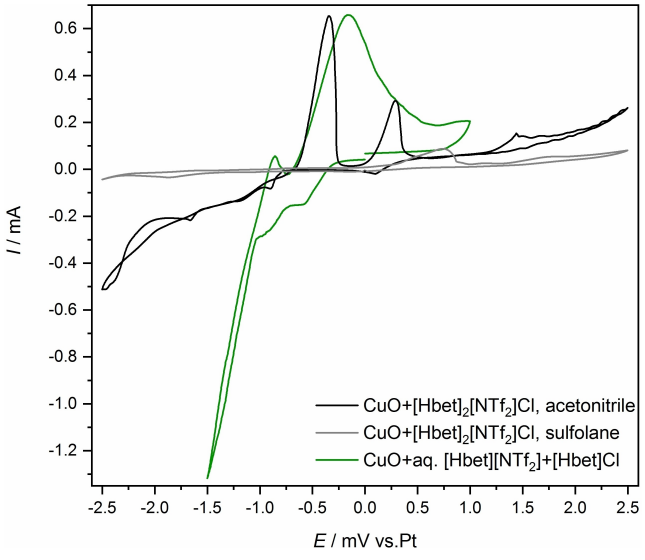

Figure 7. CVs of chloride-rich copper(II) oxide-[Hbet][NTf_2] mixtures diluted with acetonitrile or sulfolane (C) and aqueous IL (D), recorded at room temperature at a scan rate of 10 mV/s.

Copper coatings of differing appearance were obtained from several solutions. Images of the steel electrodes after the electrodeposition experiments are shown in Figure 8.

In the aqueous sample (D), copper formation occurred directly upon immersing the steel electrode into the solution without applying any potential. The copper deposit adheres only loosely to the steel surface, and copper flakes (PXRD in Figure S8) start to diffuse through the solution. When rinsing with acetone the most of the coating is lost (see also the energy-dispersive X-ray spectroscopy (EDX) maps of the local element distribution, Figure S9). As copper has a higher electrochemical potential,[89] iron dissolves in a copper(II) solution upon simultaneous copper deposition. This is in agreement with the uneven, damaged electrode surface shown in Figure 9(g). Therefore, solution (D) seems unsuitable for controlled copper coating.

From the water- and solvent-free sample (E), a copper coating is obtained within 30 minutes at a potential at −0.5 V. Due to the high viscosity of the sample, elevated temperatures had to be applied. At 60 °C, the sample was still a thick paste giving no deposit. However, copper coating could be performed at 100 °C. The deposit appears slightly granular, which is confirmed by scanning electron microscopy [SEM, Figure 9(h)]. Dark, isolated spots of different shapes are present on the

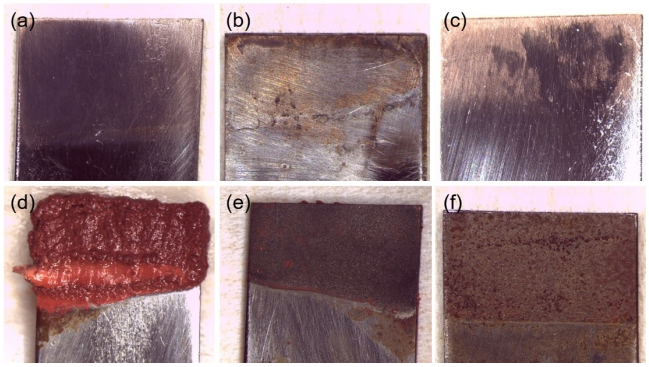

Figure 8. Copper-coated steel electrodes from copper(II) oxide and [Hbet][NTf_2] (a) in sulfolane [sample (B)], (b) with [Hbet]Cl in sulfolane [sample (C)], (c) with [Hbet]Cl in acetonitrile [sample (C)], (d) with [Hbet]Cl in aqueous solution before and (e) after rinsing [sample (D)], (f) with [Hbet]Cl solvent-free [sample (E)].

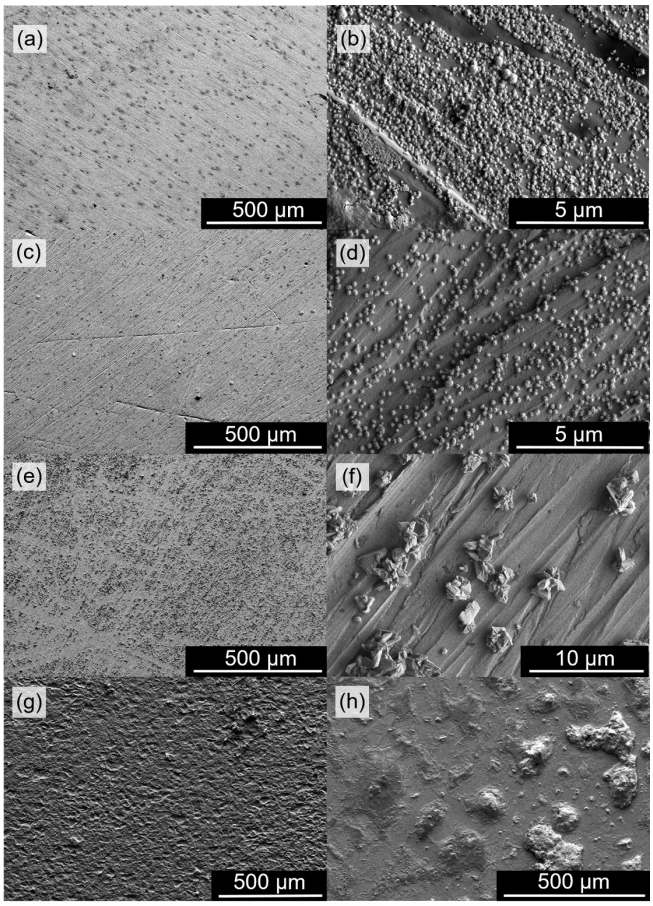

Figure 9. SEM images of the electrode surface (a), (b) CuO and [Hbet][NTf_2] in sulfolane [sample (C)], (c), (d) CuO, [Hbet][NTf_2] and [Hbet]Cl in sulfolane [sample (C)], (e), (f) CuO, [Hbet][NTf_2] and [Hbet]Cl in acetonitrile [sample (C)], (g) CuO, aqueous [Hbet][NTf_2] and [Hbet]Cl [sample (D)], (h) CuO, [Hbet][NTf_2] and [Hbet]Cl solvent-free [sample (E)].

electrode surface. EDX maps of the local element distribution detect only a small amount of copper in these isles, although an even distribution in between (Figure S10). This is in agreement with more precise EDX point measurements shown in Figures S11 and S12. From these results, it is assumed that copper is deposited as a relatively even coating, but organic material crystallizes as well in a spotty way. This is not surprising considering the negligible excess of IL that would be able to dissolve organic material released from copper complexes. The EDX point measurements in Figure S11 suggest chloride-rich compounds in the isles. Due to the low amount of deposit obtained in the coating experiment, the organic material, could not be characterized by PXRD, yet. Further experiments with varying sample composition, especially an excess of [Hbet][NTf_2], should be conducted as an increased amount of the IL could lower the reaction temperature and might prevent the deposition of organic material.

In contrast to that, the copper deposition from diluted solutions, i.e. sample (B) and (C) in acetonitrile or sulfolane, appears to be inhibited. No deposits are obtained by gradually decreasing the potential to −2.5 V. Not until a potential of −3.0 V was applied for 30 minutes, thin, copper-colored coatings were observed from the solutions of CuO and [Hbet][NTf_2] (B) in sulfolane as well as CuO, [Hbet][NTf_2] and [Hbet]Cl (C) in sulfolane or acetonitrile [Figure 8(a)–(c)]. However, no deposition occurred in sample (B) in acetonitrile. EDX maps of the local element distribution confirm that the obtained deposits consist of copper, alongside with some organic material (Figures S13–S15). SEM images of sample (B) and (C) in sulfolane show relatively uniform copper coatings [Figure 9(a)–(d)]. Spherical copper particles, mostly smaller than 100 nm, are distributed at the steel surfaces. In the sample of CuO and [Hbet][NTf_2] (B), these particles are more densely packed, while other areas of the steel surface remain bare. Furthermore, the particle size distribution is broader. The chloride-rich sample (C) displays more homogenous particles regarding their size and distribution. Apparently, complex speciation in the sulfolane solutions affects the growth of particles on the steel surface. In contrast to this, the copper deposit from the chloride-rich sample (C) dissolved in acetonitrile is more inhomogeneous. Particles of various shapes and sizes of several micrometers are distributed relatively unevenly on the steel surface [Figure 9(e), (f)]. This suggests that the electrodeposition of copper from acetonitrile is less favored on steel. After the initial deposition of copper particles on the electrode surface, further reduction might preferably take place on the copper substrate, increasing the particle size. Altogether, dilution with solvents appears to allow relatively uniform copper coating, whereby the solvent as well as complex speciation influence the product. However, significantly higher negative potentials compared to the solvent-free sample (E) have to be applied. An explanation could be a high overpotential on steel in the respective solvent.

To summarize, we show that copper deposition from different solutions is possible. Complex speciation as well as dilution with different solvents appears to have a significant effect on the deposition potentials as well as the properties of the copper coatings. In order to determine the optimal copper deposition strategy for a specific purpose, further investigations on the characteristics of these coatings have to be performed. Furthermore, the sample composition has to be optimized towards desired coating properties. Future work should also include investigations regarding the recyclability of the IL as [Hbet][NTf_2] is the most expensive component in the process. There are promising options for the recycling of [Hbet][NTf_2] in general, as metal ions can be leached by protonating the betaine ligands.[90] If other solvents are used, the additional step of their separation is necessary, whereas several methods are possible.[91] A volatile solvent, such as acetonitrile, might be distilled. For a high-boiling solvent like sulfolane, membrane-based methods could be applicable. Finding and optimizing a suitable process involves a lot of experimental work in the future.

3. Conclusions

The dissolution of copper(II) oxide in the IL [Hbet][NTf_2] was investigated in detail. Dependent on the reaction conditions, such as chloride content, reaction temperature and impurities,

different complex species are observed. The four crystal structures discussed herein show that chloride acts as additional ligand under certain reaction conditions.

Furthermore, a mechanism for the previously reported decomposition of [Hbet][NTf_2] in the presence of chloride is suggested, which is supported by experimental evidence for chlorine and carbon dioxide as well as IR spectroscopy. It combines aspects of the Deacon process and the Hunsdieker reaction.

The electrochemical investigations show, that metal deposition from metal-betaine complexes depends on various factors. Different complex species not only affect electrochemical potentials and the characteristics of metal deposits, but also the manageability of the sample. The coatings on the steel surface were analyzed by SEM and EDX measurements, confirming the deposition of copper. Furthermore, a strong dependence on the quality of the coating from sample solution composition is found. In this work, we demonstrate the general feasibility of copper deposition from [Hbet][NTf_2], however, more investigations in this system, especially regarding the recyclability of the IL, are necessary in order to optimize the process. A low viscosity as well as inhibited crystallization and decomposition of the IL appear to be important criteria for this purpose. This could be further developed to an alternative to classical copper electroplating, starting from CuO instead of refined copper.

Altogether, this work highlights the importance of a detailed understanding of the investigated metal-betaine system, in order to realize targeted electrochemical reprocessing.

Experimental Section

Chemicals

[Hbet]Cl (99%) and copper(II) oxide (99.995%) were obtained from Alfa Aesar. Li[NTf_2] (80% aqueous solution) was purchased from iolitec. Acetonitrile (<30 ppm H_2O) was obtained from VWR chemicals and sulfolane (99%) from Merck. Copper(II) oxide (97.5%) was obtained from Roth. In order to determine whether copper(I) oxide is contained in the 2.5% impurities, the reagent was heated in an oxygen stream. As thermogravimetric analysis of copper(I) oxide in air suggested the completion of mass gain at 470 °C, 500 °C was chosen as oxidation temperature. Copper(II) oxide (97.5%) was flushed with oxygen in a glass tube for 16 hours, subsequently, the temperature was elevated at $\Delta T/t = 300\,K\,h^{-1}$, kept at 500 °C for 6 h and cooled down overnight.

Synthesis of [Hbet][NTf_2]

[Hbet][NTf_2] was synthesized according to a literature procedure[33] by stirring 0.1 mol [Hbet]Cl dissolved in 50 ml water and 0.1 mol Li[NTf_2] solution for one hour. Subsequently, the IL was separated and washed with ice-cold water until chloride ions could not be detected anymore by testing with $AgNO_3$ solution, typically five times. The IL was dried under vacuum at a rotary evaporator at 60 °C for one hour and under dynamic vacuum of 10^{-2} mbar at 110 °C overnight.

Synthesis of $[Cu_2(bet)_4(NTf_2)_2][NTf_2]_2$

1 was obtained according to a previously described synthesis[35] by stirring copper(II) oxide (99.995% or 97.5%) and [Hbet][NTf_2] in a molar ratio of 1:2 with the addition of 0.3 mol% [Hbet]Cl. The reaction was performed in an open round bottom flask at 175 °C for 24 h. Blue crystals of several shapes were obtained directly after the reaction.

Synthesis of $[Cu(bet)_4]_2[N(CH_3)_3(CH_2Cl)][NTf_2]_5$

Compound **2** was synthesized by heating copper(II) oxide (99.995%), [Hbet][NTf_2] and [Hbet]Cl in a molar ratio of 1:2:2 to 175 °C for 4 h in a system open to the air. Blue, rod-like crystals up to a length of 2 mm were obtained after one day at room temperature.

Synthesis of $[Cu_3(bet)_4Cl_3][NTf_2]_3$

3 was obtained by storing a mixture of copper(II) oxide (99.995%), [Hbet][NTf_2] and [Hbet]Cl in a molar ratio of 1:6:1 at room temperature in an open vessel for 9 months. Amongst others, blue crystals were found when investigating the sample under the microscope.

Synthesis of $[Cu_2(bet)_4][Cu_6Cl_{10}]$

4 was obtained in the same reaction like **2** when using copper(II) oxide of 97.5% purity. Copper(II) oxide (97.5%), [Hbet][NTf_2] and [Hbet]Cl in a molar ratio of 1:2:2 were heated to 175 °C for 4 h in a system open to the air. Some small, blue, block-like crystals were present directly after the reaction, which grew and increased in number during one day at room temperature.

Comment on the Thermal Behavior of Compounds 1–4

Melting or decomposition points of new coordination compounds can be valuable information.[33] However, as the complexes reported herein were not synthesized as single phase materials, this is difficult to realize. First of all, the individual crystals cannot be separated as no solvent only for the IL (and other compounds present) was found. A rough estimation of the thermal behaviour was performed by gently cleaning selected crystals from some adherent IL with fuzz-free paper and heating in 10 K steps for 30 minutes each. Optical investigation indicates that **1** decomposes between 240 °C and 270 °C without prior melting, which is in agreement with thermal analysis. For compounds **2**, **3** and **4**, it is not clear whether they melt or re-dissolve in the adherent IL before they decompose. Thermal analysis was not performed as the assignment of signals to a specific compound in a sample of unknown phase composition would be mere speculation.

X-Ray Crystal Structure Determination

The collection of diffraction intensities of single-crystals was performed on a Kappa APEX II CCD diffractometer (Bruker) with Mo-K_α radiation ($\lambda = 71.073$ pm) at 100(2) K under flowing nitrogen gas. Empirical multi-scan absorption corrections were applied to the data. Structure solution was done with the program SHELXT[92] in OLEX2[93] via intrinsic phasing. Structure refinement was performed with the method of full-matrix least squares on F_0^2 with the program SHELXL[92,94] in OLEX2.[93] Non-hydrogen atoms were refined with anisotropic displacement parameters, hydrogen atoms were refined with riding coordinates and displacement parameters.

The crystal structures were plotted in the program Diamond.[95] The full crystallographic data is deposited at the Cambridge Crystallographic Data Centre, deposit numbers CCDC 1947513 (**1**), CCDC 2021280 (**2**), CCDC 2021283 (**3**) and CCDC 2021281 (**4**).

$[Cu(bet)_4]_2[N(CH_3)_3(CH_2Cl)][NTf_2]_5$: monoclinic space group $P2_1/n$ (no. 14); $T=100(2)$ K; $a=2109.56(9)$ pm, $b=2232.56(9)$ pm, $c=2181.44(9)$ pm, $\beta=90.633(1)^\circ$, $V=10273.3(7)\times10^6$ pm^3; $Z=4$; $\rho_{calc}=1.664$ g cm^{-3}; μ(Mo-K$_\alpha$)$=0.780$ mm^{-1}; $2\theta_{max}=56.6^\circ$, $-28\le h\le28$, $-29\le k\le29$, $-29\le l\le29$; 329240 measured, 25608 unique reflections, $R_{int}=0.048$, $R_\sigma=0.023$; 1312 parameters, R_1[20389 $F_o>4\sigma(F_o)$]$=0.060$, wR_2(all F_o^2)$=0.170$, $GooF=1.165$, residual electron density -1.95 to 5.50 e$\times10^{-6}$ pm^{-3}. The description of the disorder of one of the $[NTf_2]^-$ anions uses two conformations, yet the residual electron density indicates additional non-modelled disorder. For selected interatomic distances, see Table S1.

$[Cu_3(bet)_4Cl_3][NTf_2]_3$: orthorhombic space group $Cmc2_1$ (no. 36); $T=100(2)$ K; $a=2504.27(9)$ pm, $b=1661.29(6)$ pm and $c=1342.53(5)$ pm, $V=5585.4(4)\times10^6$ pm^3; $Z=4$; $\rho_{calc}=1.910$ g cm^{-3}; μ(Mo-K$_\alpha$)$=1.633$ mm^{-1}; $2\theta_{max}=73.0^\circ$, $-41\le h\le41$, $-27\le k\le27$, $-22\le l\le22$; 194841 measured, 13863 unique reflections, $R_{int}=0.065$, $R_\sigma=0.034$; 443 parameters, R_1[12473 $F_o>4\sigma(F_o)$]$=0.031$, wR_2(all F_o^2)$=0.065$, $GooF=1.055$, residual electron density -1.17 to 0.76 e$\times10^{-6}$ pm^{-3}. One of the non-mirror-symmetric $[NTf_2]^-$ anions is positioned in the mirror plane *m*. This involves large anisotropic displacement parameters of the individual atoms and split positions for the sulfur atoms. For selected interatomic distances, see Table S2.

$[Cu_2(bet)_4][Cu_6Cl_{10}]$: monoclinic space group $P2_1/n$ (no. 14); $T=100(2)$ K; $a=1516.32(14)$ pm, $b=906.38(8)$ pm, $c=1652.66(16)$ pm and $\beta=113.018(3)^\circ$, $V=2090.5(3)\times10^6$ pm^3; $Z=4$; $\rho_{calc}=2.115$ g cm^{-3}; μ(Mo-K$_\alpha$)$=4.670$ mm^{-1}; $2\theta_{max}=55.5^\circ$, $-19\le h\le19$, $-11\le k\le11$, $-21\le l\le21$; 101058 measured, 4870 unique reflections, $R_{int}=0.106$, $R_\sigma=0.039$; 269 parameters, R_1[3511 $F_o>4\sigma(F_o)$]$=0.053$, wR_2(all F_o^2)$=0.123$, $GooF=1.025$, residual electron density -1.39 to 2.33 e$\times10^{-6}$ pm^{-3}. The atoms of the betaine ligands show a relatively high mobility, indicated by large displacement ellipsoids suggesting disorder. To restrict the complexity of the structure model, split positions were refined for two oxygen atoms and one carbon atom in equal partial amounts. Furthermore, for one chloride atom, two minor split positions [occupation 0.106(3) and 0.064(3)] were refined. For selected interatomic distances, see Table S3.

Cyclic Voltammetry

For CV measurements, (A) 500 mg [Hbet][NTf_2], (B) 50 mg copper(II) oxide, 500 mg [Hbet][NTf_2] and 1 mg [Hbet]Cl (molar ratio 1:2:0.02, 24 h at 175 °C) and (C) 50 mg copper(II) oxide, 500 mg [Hbet][NTf_2] and 193 mg [Hbet]Cl (molar ratio 1:2:2, 4 h at 175 °C) were dissolved in 25 ml acetonitrile or sulfolane. For another sample (D), 35 ml aqueous [Hbet][NTf_2] was synthesized according to *Nockemann* et al.[33] without drying. Then, 400 mg copper(II) oxide and 770 mg [Hbet]Cl (molar ratio 1:1) were dissolved by stirring at room temperature for 16 h, yielding a blue-green solution. CV measurements were performed in a three-electrode electrochemical cell with a glassy carbon disk working electrode (diameter 3 mm), a platinum wire as counter electrode and a platinum plate as pseudo-reference electrode in the range of −2.5 V to 2.5 V and with a scan rate of 10 mV/s. The measuring range for sample (D) was −1.5 V to 1.0 V. Prior to the measurement, the platinum electrodes were rinsed with acetone and cleaned with fuzz-free tissue, before drying on air. The working electrode was polished with 0.05 µm alumina paste on a velvet pad, subsequently rinsed with acetone and dried on air.

Electrochemical copper deposition

Prior to electrodeposition experiments, according to literature,[96] steel plates (width 10 mm, length 20 mm) were mechanically polished with increasingly fine SiC paper (P320, P1200, P2500). Subsequently, the steel substrate was ultrasonically cleaned in acetone for 15 minutes, followed by drying at 110 °C for 30 minutes. The effectivity of this cleaning procedure is proven by SEM images in Figure S6. For electrodeposition experiments, six solutions were prepared: (B) 50 mg copper(II) oxide, 500 mg [Hbet][NTf_2] and 1 mg [Hbet]Cl (molar ratio 1:2:0.02, 24 h at 175 °C) in 25 ml acetonitrile or sulfolane, (C) 50 mg copper(II) oxide, 500 mg [Hbet][NTf_2] and 193 mg [Hbet]Cl (molar ratio 1:2:2, 4 h at 175 °C) in 25 ml acetonitrile or sulfolane, (D) 400 mg copper(II) oxide and 770 mg [Hbet]Cl (molar ratio 1:1) in 35 ml aqueous [Hbet][NTf_2], (E) 300 mg copper(II) oxide, 3 g [Hbet][NTf_2] and 1.16 g [Hbet]Cl (molar ratio 1:2:2, 4 h at 175 °C). A steel plate was placed in sample (D) for 30 minutes without any potential applied. For the other samples, a simple two-electrode setup was used with a steel working electrode and a platinum wire as counter electrode. A voltage of −500 mV was applied for 30 minutes at 100 °C for sample (E). For (B) and (C), the voltage was decreased from −0.5 V to −3.0 V in steps of 0.5 V (30 minutes each) at room temperature.

Powder X-Ray Diffractometry

PXRD was performed on an Empyrean diffractometer (PANanalytical) equipped with a curved Ge(111) monochromator in Bragg–Brentano geometry at 296 K using Cu-$K_{\alpha1}$ radiation ($\lambda=154.056$ pm).

Scanning Electron Microscopy and Energy-dispersive X-ray Spectroscopy

For SEM and EDX measurements, the steel electrodes were adhered to the sample holder. Scanning electron microscopy ($U_a=2$ kV) and semi-quantitative energy-dispersive X-ray spectroscopy ($U_a=20$ kV) were performed using a SU8020 electron microscope (Hitachi) equipped with an Oxford Silicon Drift Detector X-Max^N.

Acknowledgements

We thank Alexander Purtsas for discussion, Maria Herz for SEM and EDX measurements, Daniel Spittel for providing the glassy carbon electrode and Michaela Münch for technical support. Furthermore, we are grateful to an unknown referee for very helpful comments. This research was supported by the German Research Foundation (DFG) within the framework of the Priority Program SPP 1708.

Conflict of Interest

The authors declare no conflict of interest.

Keywords: copper · coordination compounds · electrodeposition · Hunsdieker reaction · ionic liquids

[1] A. F. Holleman, E. Wiberg, N. Wiberg, G. Fischer, *Anorganische Chemie*, De Gruyter, Berlin Boston, **2017**.

[2] P. Davris, E. Balomenos, D. Panias, I. Paspaliaris, *Light Metals 2018* (Ed.: O. Martin), Springer International Publishing, Cham, **2018**, pp. 149–156.
[3] D. Dupont, K. Binnemans, *Green Chem.* **2015**, *17*, 856–868.
[4] M. Orefice, K. Binnemans, T. Vander Hoogerstraete, *RSC Adv.* **2018**, *8*, 9299–9310.
[5] F.-L. Fan, Z. Qin, S.-W. Cao, C.-M. Tan, Q.-G. Huang, D.-S. Chen, J.-R. Wang, X.-J. Yin, C. Xu, X.-G. Feng, *Inorg. Chem.* **2019**, *58*, 603–609.
[6] G. Damilano, A. Laitinen, P. Willberg-Keyriläinen, T. Lavonen, R. Häkkinen, W. Dehaen, K. Binnemans, L. Kuutti, *RSC Adv.* **2020**, *10*, 23484–23490.
[7] S. Wellens, N. R. Brooks, B. Thijs, L. V. Meervelt, K. Binnemans, *Dalton Trans.* **2014**, *43*, 3443–3452.
[8] S. Wellens, T. Vander Hoogerstraete, C. Möller, B. Thijs, J. Luyten, K. Binnemans, *Hydrometallurgy* **2014**, *144–145*, 27–33.
[9] D. Dupont, E. Renders, K. Binnemans, *Chem. Commun.* **2016**, *52*, 4640–4643.
[10] D. Dupont, E. Renders, S. Raiguel, K. Binnemans, *Chem. Commun.* **2016**, *52*, 7032–7035.
[11] I. Billard, C. Gaillard, C. Hennig, *Dalton Trans.* **2007**, 4214–4221.
[12] B. Zhang, Y. Yao, Z. Shi, J. Xu, Z. Wang, *ChemElectroChem* **2018**, *5*, 3368–3372.
[13] C. A. Zarzana, G. S. Groenewold, M. T. Benson, J. E. Delmore, T. Tsuda, R. Hagiwara, *J. Am. Soc. Mass Spectrom.* **2018**, *29*, 1963–1970.
[14] C. J. Rao, K. A. Venkatesan, K. Nagarajan, T. G. Srinivasan, *Radiochim. Acta* **2008**, *96*, 403–409.
[15] A. P. Abbott, G. Capper, D. L. Davies, K. J. McKenzie, S. U. Obi, *J. Chem. Eng. Data* **2006**, *51*, 1280–1282.
[16] N. Rodriguez Rodriguez, L. Machiels, K. Binnemans, *ACS Sustainable Chem. Eng.* **2019**, *7*, 3940–3948.
[17] A. P. Abbott, G. Capper, D. L. Davies, R. K. Rasheed, P. Shikotra, *Inorg. Chem.* **2005**, *44*, 6497–6499.
[18] W. Chen, J. Jiang, X. Lan, X. Zhao, H. Mou, T. Mu, *Green Chem.* **2019**, *17*, 4748–4756.
[19] S. M. Shuwa, R. S. Al-Hajri, B. Y. Jibril, Y. M. Al-Waheibi, *Ind. Eng. Chem. Res.* **2015**, *54*, 3589–3601.
[20] J. Ru, Y. Hua, C. Xu, J. Li, Y. Li, D. Wang, C. Qi, K. Gong, *Russ. J. Electrochem.* **2015**, *51*, 773–781.
[21] H. Yang, R. G. Reddy, *J. Electrochem. Soc.* **2014**, *161*, D586–D592.
[22] P. Billik, P. Antal, R. Gyepes, *Inorg. Chem.* **2015**, *60*, 37–40.
[23] H. Yang, R. G. Reddy, *Electrochim. Acta* **2015**, *178*, 617–623.
[24] J. Richter, M. Ruck, *Molecules* **2020**, *25*, 78.
[25] P. Wasserscheid (Ed.), *Ionic Liquids in Synthesis*, Wiley-VCH, Weinheim, **2002**
[26] P. Mahjoor, S. E. Latturner, *Cryst. Growth Des.* **2009**, *9*, 1385–1389.
[27] S. Dai, Y. S. Shin, L. M. Toth, C. E. Barnes, *Inorg. Chem.* **1997**, *36*, 4900–4902.
[28] R. C. Bell, A. W. Castleman, D. L. Thorn, *Inorg. Chem.* **1999**, *38*, 5709–5715.
[29] E. Wanigasekara, J. W. Freiderich, X.-G. Sun, R. A. Meisner, H. Luo, L. H. Delmau, S. Dai, B. A. Moyer, *Dalton Trans.* **2016**, *45*, 10151–10154.
[30] P. Nockemann, B. Thijs, T. N. Parac-Vogt, K. Van Hecke, L. Van Meervelt, B. Tinant, I. Hartenbach, T. Schleid, V. T. Ngan, M. T. Nguyen, K. Binnemans, *Inorg. Chem.* **2008**, *47*, 9987–9999.
[31] D. Dupont, S. Raiguel, K. Binnemans, *Chem. Commun.* **2015**, *51*, 9006–9009.
[32] P. Mäkelä, *Sugar Tech* **2004**, *6*, 207–212.
[33] P. Nockemann, B. Thijs, S. Pittois, J. Thoen, C. Glorieux, K. Van Hecke, L. Van Meervelt, B. Kirchner, K. Binnemans, *J. Phys. Chem. B* **2006**, *110*, 20978–20992.
[34] P. Nockemann, B. Thijs, K. V. Hecke, L. V. Meervelt, K. Binnemans, *Cryst. Growth Des.* **2008**, *8*, 1353–1363.
[35] J. Richter, M. Ruck, *RSC Adv.* **2019**, *9*, 29699–29710.
[36] T. Fuchigami, S. Inagi, M. Atobe, Eds., *Fundamentals and Applications of Organic Electrochemistry*, John Wiley & Sons Ltd, Chichester, U. K., **2014**.
[37] S. Creager, *Handbook of Electrochemistry*, Elsevier, **2007**, pp. 57–72.
[38] J. Zhang, A. M. Bond, *Analyst* **2005**, *130*, 1132–1147.
[39] H. Matsumoto, in *Electrochemical Aspects of Ionic Liquids* (Ed.: H. Ohno), John Wiley & Sons, Inc., Hoboken, NJ, USA, **2005**, pp. 35–54.
[40] H.-W. Yeh, Y.-H. Tang, P.-Y. Chen, *J. Electrochem. Soc.* **2018**, *811*, 68–77.
[41] T. Tsuda, L. E. Boyd, S. Kuwabata, C. L. Hussey, *J. Electrochem. Soc.* **2010**, *157*, F96–F103.
[42] X. Xie, X. Zou, X. Lu, Q. Xu, C. Lu, C. Chen, Z. Zhou, *J. Appl. Electrochem.* **2017**, *47*, 679–689.
[43] P. Huang, Y. Zhang, *Int. J. Electrochem. Sci.* **2018**, *13*, 10798–10808.
[44] J. Ru, Y. Hua, C. Xu, J. Li, Y. Li, D. Wang, C. Qi, Y. Jie, *Appl. Surf. Sci.* **2015**, *335*, 153–159.
[45] H. Yang, R. G. Reddy, *Electrochim. Acta* **2014**, *147*, 513–519.
[46] A. Liu, Z. Shi, R. G. Reddy, *J. Electrochem. Soc.* **2017**, *164*, D666–D673.
[47] W. He, L. Shen, Z. Shi, B. Gao, X. Hu, J. Xu, Z. Wang, *Electrochemistry* **2016**, *84*, 872–877.
[48] Y. Zheng, K. Dong, Q. Wang, S. Zhang, Q. Zhang, X. Lu, *Sci. China Chem.* **2012**, *55*, 1587–1597.
[49] K. Jayachandran, R. Gupta, K. R. S. Chandrakumar, D. Goswami, D. M. Noronha, S. Paul, S. Kannan, *Chem. Commun.* **2019**, *55*, 1474–1477.
[50] L. J. Durney, in *Ullmann's Encyclopedia of Industrial Chemistry* (Ed.: Wiley-VCH Verlag GmbH & Co. KGaA), Wiley-VCH Verlag GmbH & Co. KGaA, Weinheim, Germany, **2000**.
[51] N. Kanani, *Galvanotechnik: Grundlagen, Verfahren und Praxis einer Schlüsseltechnologie*, Hanser, München, **2009**.
[52] European Commission, *Integrated Pollution Prevention and Control. Reference Document on Best Available Techniques for the Surface Treatment of Metals and Plastics* **2006**, 14–15, 41–43.
[53] F. Endres, A. Schweizer, *Phys. Chem. Chem. Phys.* **2000**, *2*, 5455–5462.
[54] P.-Y. Chen, I.-W. Sun, *Electrochim. Acta* **1999**, *45*, 441–450.
[55] C. Rousse, S. Beaufils, P. Fricoteaux, *Electrochim. Acta* **2013**, *107*, 624–631.
[56] S. Anggara, F. Bevan, R. C. Harris, J. M. Hartley, G. Frisch, G. R. T. Jenkin, A. P. Abbott, *Green Chem.* **2019**, *21*, 6502–6512.
[57] P. Nockemann, B. Thijs, K. Lunstroot, T. N. Parac-Vogt, C. Görller-Walrand, K. Binnemans, K. Van Hecke, L. Van Meervelt, S. Nikitenko, J. Daniels, C. Hennig, R. Van Deun, *Chem. Eur. J.* **2009**, *15*, 1449–1461.
[58] Y.-X. Mei, X.-N. Hua, J.-X. Gao, W.-Q. Liao, *CrystEngComm* **2018**, *20*, 6261–6266.
[59] X.-N. Hua, C.-R. Huang, J.-X. Gao, Y. Lu, X.-G. Chen, W.-Q. Liao, *Dalton Trans.* **2018**, *47*, 6218–6224.
[60] W.-Q. Liao, J.-X. Gao, X.-N. Hua, X.-G. Chen, Y. Lu, *J. Mater. Chem. C* **2017**, *5*, 11873–11878.
[61] X.-N. Hua, W.-Q. Liao, Y.-Y. Tang, P.-F. Li, P.-P. Shi, D. Zhao, R.-G. Xiong, *J. Am. Chem. Soc.* **2018**, *140*, 12296–12302.
[62] Y.-M. You, W.-Q. Liao, D. Zhao, H.-Y. Ye, Y. Zhang, Q. Zhou, X. Niu, J. Wang, P.-F. Li, D.-W. Fu, Z. Wang, S. Gao, K. Yang, J.-M. Liu, J. Li, Y. Yan, R.-G. Xiong, *Science* **2017**, *357*, 306–309.
[63] D. Li, X.-M. Zhao, H.-X. Zhao, L.-S. Long, L.-S. Zheng, *Inorg. Chem.* **2019**, *58*, 655–662.
[64] A. Sieker, A. J. Blake, B. F. G. Johnson, *J. Chem. Soc. Dalton Trans.* **1996**, 1419–1427.
[65] H. Deacon, *J. Chem. Soc.* **1872**, *25*, 725–767.
[66] H. Hunsdiecker, C. Hunsdiecker, *Ber. Dtsch. Chem. Ges. A, B* **1942**, *75*, 291–297.
[67] C. V. Wilson, in *Organomet. React.* (Ed.: John Wiley & Sons, Inc.), John Wiley & Sons, Inc., Hoboken, NJ, USA, **2011**, pp. 332–387.
[68] R. G. Johnson, R. K. Ingham, *Chem. Rev.* **1956**, *56*, 219–269.
[69] F. Endres, S. Z. El Abedin, N. Borissenko, *Z. Phys. Chem.* **2006**, *220*, 1377–1394.
[70] M. A. Abdalrahman, F. F. Awwadi, G. B. Jameson, C. P. Landee, C. G. Saunders, M. M. Turnbull, J. L. Wikaira, *CrystEngComm* **2013**, *15*, 4309–4320.
[71] S. K. Hota, C. R. Saha, H. Pritzkow, *J. Coord. Chem.* **1984**, *13*, 131–142.
[72] R. J. Williams, D. T. Cromer, W. H. Watson, *Acta Crystallogr. Sect. B* **1971**, *27*, 1619–1624.
[73] D. Braga, F. Grepioni, L. Maini, R. Brescello, L. Cotarca, *CrystEngComm* **2008**, *10*, 469–471.
[74] M. R. Silva, J. A. Paixão, A. M. Beja, L. A. da Veiga, J. Martín-Gil, *J. Chem. Crystallogr.* **2001**, *31*, 167–171.
[75] N. E. Brese, M. O'Keeffe, *Acta Crystallogr. Sect. B* **1991**, *47*, 192–197.
[76] W. Clegg, J. R. Nicholson, D. Collison, C. D. Garner, *Acta Crystallogr. Sect. C* **1988**, *44*, 453–461.
[77] Z. Xing, H.-B. Yin, *Z. Kristallogr. New Cryst. Struct.* **2019**, *234*, 391–392.
[78] M. Asplund, S. Jagner, P.-E. Werner, M. Westdahl, *Acta Chem. Scand.* **1984**, *38a*, 807–811.
[79] S. Link, S. Ivanov, A. Dimitrova, S. Krischok, A. Bund, *Electrochem. Commun.* **2019**, *103*, 7–11.
[80] S. Fletcher, I. Kirkpatrick, R. Thring, R. Dring, J. L. Tate, H. R. M. Geary, V. J. Black, *ACS Sustainable Chem. Eng.* **2018**, *6*, 2612–2620.
[81] F. P. Byrne, S. Jin, G. Paggiola, T. H. M. Petchey, J. H. Clark, T. J. Farmer, A. J. Hunt, C. Robert McElroy, J. Sherwood, *Sustainable Chem. Processes* **2016**, *4*, DOI 10.1186/s40508-016-0051-z.
[82] U. Tilstam, *Org. Process Res. Dev.* **2012**, *16*, 1273–1278.

[83] A. Bak, V. Kozik, P. Dybal, S. Kus, A. Swietlicka, J. Jampilek, *Sustainability* **2018**, *10*, 3677.
[84] K. Wang, J. Jiang, X. Liang, H. Wu, J. Xu, *ACS Sustainable Chem. Eng.* **2018**, *6*, 15092–15099.
[85] N. Teng, J. Ni, H. Chen, Q. Ren, H. Na, X. Liu, R. Zhang, J. Zhu, *ACS Sustainable Chem. Eng.* **2016**, *4*, 1507–1511.
[86] A. P. Abbott, K. J. McKenzie, *Phys. Chem. Chem. Phys.* **2006**, *8*, 4265–4279.
[87] B. A. Taleatu, E. A. A. Arbab, G. T. Mola, *Appl. Phys. A* **2015**, *120*, 959–965.
[88] B. A. Taleatu, E. Omotoso, C. Lal, W. O. Makinde, K. T. Ogundele, E. Ajenifuja, A. R. Lasisi, M. A. Eleruja, G. T. Mola, *Surf. Interface Anal.* **2014**, *46*, 372–377.
[89] D. R. Lide, in *CRC Handbook of Chemistry and Physics, Internet Version 2005*, CRC Press, Boca Raton, Florida, **2005.**
[90] D. Dupont, K. Binnemans, *Green Chem.* **2015**, *17*, 2150–2163.
[91] E. Sklavounos, J. K. J. Helminen, L. Kyllönen, I. Kilpeläinen, A. W. T. King, in *Encyclopedia of Inorganic and Bioinorganic Chemistry* (Ed.: R. A. Scott), John Wiley & Sons, Ltd, Chichester, UK, **2016**, pp. 1–16.
[92] G. M. Sheldrick, *Acta Crystallogr. Sect. A* **2008**, *64*, 112–122.
[93] *OLEX2 v1.2*, OlexSys LTd., Durham, UK, **2014**.
[94] G. M. Sheldrick, *Acta Crystallogr. Sect. C* **2015**, *71*, 3–8.
[95] K. Brandenburg, *Diamond v. 4.5.2, Crystal and Molecular Structure Visualization*, Crystal Impact GbR., Bonn, Germany, Bonn, Germany, **2018**.
[96] N. N. Che Isa, Y. Mohd, M. H. Mohd Zaki, A. A. Syed Mohamad, *Int. J. Electrochem. Sci.* **2017**, 6010–6021.

Manuscript received: August 17, 2020
Revised manuscript received: November 5, 2020